

Anatomical Predictions using Subject-Specific Medical Data

Marianne Rakic¹

MRAKIC@MIT.EDU

¹ CSAIL, MIT

John Guttag¹

GUTTAG@MIT.EDU

Adrian V. Dalca^{1,2}

ADALCA@MIT.EDU

² MGH, HMS

Abstract

Changes over time in brain anatomy can provide important insight for treatment design or scientific analyses. We present a method that predicts how a brain MRI for an individual will change over time. We model changes using a diffeomorphic deformation field that we predict using function using convolutional neural networks. Given a predicted deformation field, a baseline scan can be warped to give a prediction of the brain scan at a future time. We demonstrate the method using the ADNI cohort, and analyze how performance is affected by model variants and the subject-specific information provided. We show that the model provides good predictions and that external clinical data can improve predictions.

1. Introduction

Changes in neuroanatomy, such as brain development or neurodegeneration, are important indicators of overall health and clinical trajectory. We present a learning-based method to predict future brain anatomy from a single *baseline* MRI scan. Our method can also incorporate other clinical data; such as age, gender, and genetic information.

Longitudinal brain scan datasets have typically been used to extract correlation between brain structures and biological markers or clinical data (Biffi et al., 2010; Potkin et al., 2009; Risacher et al., 2010; Shen et al., 2010). However, providing an accurate prediction of the entire brain can give a richer phenotype for use in analysis or clinical practice. Models have been used to simulate brain evolution, taking as input one or more baseline scans. These have generally employed simple linear predictive models and had limited success (Blanc et al., 2012; Fleishman et al., 2015; Modat et al., 2014; Dalca et al., 2015). We focus on predicting the evolution of brain anatomy, using one previous scan along with external data. A recent machine learning model directly predicts future images using a black box CNN approach, without characterizing the anatomically meaningful changes (Ravi et al., 2019).

We model changes as deformations between the baseline scan and a follow-up scan, building on learning-based diffeomorphic registration methods (Balakrishnan et al., 2019; Dalca et al., 2019; de Vos et al., 2017; Ashburner, 2007; Dalca et al., 2019; Hernandez et al., 2009; Yang et al., 2017). We design a neural network that predicts such deformations and present initial results using the *ADNI II* dataset (Mueller et al., 2005a).

2. Methods

Model. Let \mathbf{x}_0 be the baseline subject brain scan, and \mathbf{a}_0 be a vector of subject-specific medical *attributes*, such as age, diagnosis, or genetic information. We predict the brain scan \mathbf{x}_t , at a later time t . We assume that evolution is captured by a deformation field $\phi_v^{(t)}$ via $\mathbf{x}_0 \circ \phi_v^{(t)}$ where \circ represents the spatial warp operation, and we obtain a noisy observation

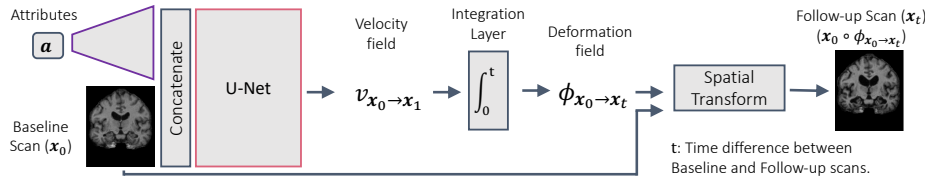


Figure 1: **Architecture.** The concatenated input scan and decoded attributes are inputs to a U-Net (Ronneberger et al., 2015), which estimates the velocity field of anatomical changes. This is then used to predict a future scan, and the predictions are compared to the true changes for longitudinal training examples to provide a loss.

\mathbf{x}_t via the likelihood: $p(\mathbf{x}_t | \phi_v^{(t)}; \mathbf{x}_0, \mathbf{a}_0) = \mathcal{N}(\mathbf{x}_t; \mathbf{x}_0 \circ \phi_v^{(t)}, \sigma^2 \mathbb{I})$, where $\mathcal{N}(\cdot; \mu, \Sigma)$ is the normal distribution with mean μ and covariance Σ , and σ^2 accounts for image noise.

We parametrize the deformations $\phi_v^{(t)}$ using a stationary velocity field, v . To encourage the predicted deformation field to be anatomically plausible, we employ a smoothness prior for the velocity field. Let \mathbf{u}_v be the displacement field such that $\phi_v = Id + \mathbf{u}_v$. Also, we let

$$p(\phi_v; \mathbf{x}_0, \mathbf{a}_0) \propto \exp\{-\gamma \|\nabla \mathbf{u}_{v_0}\|^2\}, \quad (1)$$

where γ is a parameter that regulates the importance of the priors, ∇ is the spatial differential operator, and v_0 indicates that the velocity field is a function of \mathbf{x}_0 and \mathbf{a}_0 .

The complete data likelihood is then written as:

$$p_\theta(\mathbf{x}_t; \mathbf{x}_0, \mathbf{a}_0) = \int p(\mathbf{x}_t | \phi_v^{(t)}; \mathbf{x}_0, \mathbf{a}_0) p(\phi_v^{(t)}; \mathbf{x}_0, \mathbf{a}_0) d\phi_v^{(t)}. \quad (2)$$

Learning. Because equation (2) is intractable, we use a point estimate for $\hat{\phi}_v^{(t)}$, and maximize $p(\mathbf{x}_t; \mathbf{x}_0, \mathbf{a}_0) \approx p(\mathbf{x}_t | \hat{\phi}_v^{(t)}; \mathbf{x}_0, \mathbf{a}_0)$. To obtain this point estimate, we approximate v using a neural network $g_\theta(\mathbf{x}_0, \mathbf{a}_0)$, shown Figure 1. It takes as input a baseline scan and optional clinical attributes, and outputs a velocity field, v . The network parameters, θ , are learned using stochastic gradient algorithms applied to a training dataset of longitudinal observations. Given a new pair of baseline and follow-up images $\mathbf{x}_0, \mathbf{x}_t$, we find optimal parameters θ by maximizing the posterior $\log p(\phi_v^{(t)} | \mathbf{x}_t; \mathbf{x}_0, \mathbf{a}_0)$. For each sample $\{\mathbf{x}_t, \mathbf{x}_0\}$ and predicted velocity field v , we use the loss

$$\mathcal{L}(\theta; \phi_v^{(t)}, \mathbf{x}_t, \mathbf{x}_0, \mathbf{a}_0) = -\log p(\phi_v^{(t)} | \mathbf{x}_t; \mathbf{x}_0, \mathbf{a}_0) = \frac{1}{2\sigma^2} \|\mathbf{x}_t - \mathbf{x}_0 \circ \phi_v^{(t)}\|^2 + \gamma \|\nabla \mathbf{u}_v\|^2 + cst.$$

Inference. To predict future scans, given learned parameters θ^* , we use the likelihood:

$$\mathbf{x}_t^* = \arg \max_{\mathbf{x}_t} p_{\theta^*}(\mathbf{x}_t; \mathbf{x}_0, \mathbf{a}_0), \approx \arg \max_{\mathbf{x}_t} p_{\theta^*}(\mathbf{x}_t | \phi_v^{(t)}; \mathbf{x}_0, \mathbf{a}_0),$$

following (2) and using a point estimate. We first compute $\phi_v^{(t)} = \int_0^t v dt'$ for $v = g_{\theta^*}(\mathbf{x}_0, \mathbf{a}_0)$, and then compute $\hat{\mathbf{x}}_t = \mathbf{x}_0 \circ \phi_v^{(t)}$.

3. Experiments

Data. We use the ADNI dataset (Mueller et al., 2005b) as pre-processed in (Dalca et al., 2018). For medical attributes, we select features often used in analysis: years of education, sex, APOE3, APOE4, diagnosis of the patient, and results of a Mini-Mental State Examination. Segmentation maps obtained via FreeSurfer including 29 anatomical structures are used in evaluating registration results using the Dice score and surface distance between the ground truth follow-up maps and the propagated segmentation labels.

Comparative Methods. We consider three comparative methods. The first assumes no anatomical change between the baseline and follow-up scan. The second one gives the

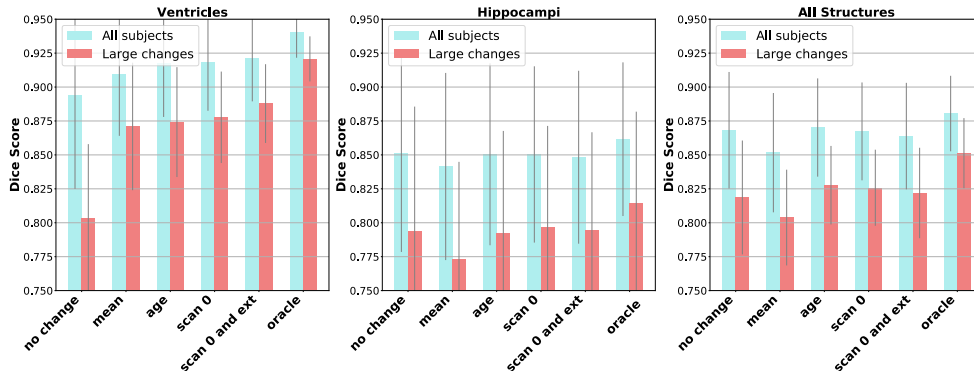


Figure 2: **Dice score evaluated for the test set.** The name of the model corresponds to the input of the network, with **ext** being the full set of external data.

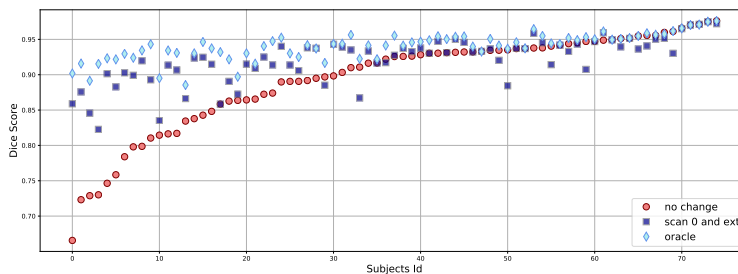


Figure 3: **Relative change of performance for the different subjects evaluated on ventricles.** The subjects are ordered by decreasing change of ventricle volume between the two scans.

deformation field obtained by integration of the average registration velocity field (mean) in the training set (Ashburner, 2007). The third (oracle) is an upper bound that uses the follow-up scan and outputs the deformation field by registering the baseline **and** the follow-up scan (Balakrishnan et al., 2018).

Model Variants. We train variants of the proposed model, with results given in Figure 2 and Figure 3. We distinguish between subjects who experience large changes between the baseline and follow-up scans and the ones that don't. We observe that the proposed model is able to significantly improve on the baselines in some structures, such as the ventricles, and come close to the upper bound. Specifically, for ventricles, adding clinical information tends to further improve the results. For other structures not affected by external data, such as the hippocampi, we hypothesize that external information is instead captured in the medical scan itself and extracted by our network. Surface distance gives similar results.

4. Conclusion

We propose a deformation model and neural network architecture for predicting anatomical changes from a single baseline scan. In initial experiments, we show that the proposed architecture can extract meaningful information and lead to promising predictions. We limit our model to shape changes to focus on modelling neurodegeneration and atrophy. It would further be interesting to determine whether predictions could be enhanced by leveraging label maps during training and by incorporating intensity changes in the model.

References

- J. Ashburner. A fast diffeomorphic image registration algorithm. *Neuroimage*, 38(1):95–113, 2007.
- G. Balakrishnan et al. An unsupervised learning model for deformable medical image registration. In *CVPR*, pages 9252–9260, 2018.
- G. Balakrishnan et al. Voxelmorph: a learning framework for deformable medical image registration. *T-MI*, 2019.
- A. Biffi et al. Genetic variation and neuroimaging measures in alzheimer disease. *Archives of neurology*, 67(6):677–685, 2010.
- R. Blanc et al. Statistical model based shape prediction from a combination of direct observations and various surrogates: application to orthopaedic research. *Medical image analysis*, 16(6):1156–1166, 2012.
- A.V. Dalca et al. Predictive modeling of anatomy with genetic and clinical data. In *MICCAI*, pages 519–526. Springer, 2015.
- A.V. Dalca et al. Anatomical priors in convolutional networks for unsupervised biomedical segmentation. In *CVPR*, pages 9290–9299, 2018.
- A.V. Dalca et al. Unsupervised learning of probabilistic diffeomorphic registration for images and surfaces. *Medical image analysis*, 57:226–236, 2019.
- B.D. de Vos et al. End-to-end unsupervised deformable image registration with a convolutional neural network. In *DLMIA*, pages 204–212. Springer, 2017.
- G.M. Fleishman et al. Simultaneous longitudinal registration with group-wise similarity prior. In *IPMI*, pages 746–757. Springer, 2015.
- M. Hernandez et al. Registration of anatomical images using paths of diffeomorphisms parameterized with stationary vector field flows. *IJCV*, 85(3):291–306, 2009.
- M. Modat et al. Simulating neurodegeneration through longitudinal population analysis of structural and diffusion weighted mri data. In *MICCAI*, pages 57–64. Springer, 2014.
- S.G. Mueller et al. The alzheimer’s disease neuroimaging initiative. *Neuroimaging Clinics*, 15(4):869–877, 2005a.
- S.G. Mueller et al. Ways toward an early diagnosis in alzheimer’s disease: the alzheimer’s disease neuroimaging initiative (adni). *Alzheimer’s & Dementia*, 1(1):55–66, 2005b.
- S.G. Potkin et al. Hippocampal atrophy as a quantitative trait in a genome-wide association study identifying novel susceptibility genes for alzheimer’s disease. *PloS one*, 4(8):e6501, 2009.
- D. Ravi et al. Degenerative adversarial neuroimage nets: Generating images that mimic disease progression. In *MICCAI*, pages 164–172. Springer, 2019.
- S.L. Risacher et al. Longitudinal mri atrophy biomarkers: relationship to conversion in the adni cohort. *Neurobiology of aging*, 31(8):1401–1418, 2010.
- O. Ronneberger et al. U-net: Convolutional networks for biomedical image segmentation. In *MICCAI*, pages 234–241. Springer, 2015.
- L. Shen et al. Whole genome association study of brain-wide imaging phenotypes for identifying quantitative trait loci in mci and ad: A study of the adni cohort. *Neuroimage*, 53(3):1051–1063, 2010.
- X. Yang et al. Quicksilver: Fast predictive image registration—a deep learning approach. *NeuroImage*, 158:378–396, 2017.